Constraining general relativity with gravitational waves

Felipe Barbosa

In collaboration with Davi C. Rodrigues, Josiel Mendonça Soares de Souza, Miguel Quartin, Michele Mancarella and Matheus F. S. Alves.

- The gravitational wave strain is defined in terms of the difference on the round trip travel time:

$$h(t) = (\Delta t^{\text{arm1}}_{\text{round trip}} - \Delta t^{\text{arm2}}_{\text{round trip}})/\Delta T,$$
$$\Delta T = \frac{2L0}{c}. \quad (1)$$

- The gravitational wave strain is defined in terms of the difference on the round trip travel time:

$$h(t) = (\Delta t^{\mathrm{arm1}}_{\mathrm{round\ trip}} - \Delta t^{\mathrm{arm2}}_{\mathrm{round\ trip}})/\Delta T,$$
$$\Delta T = \frac{2L0}{c}. \tag{1}$$

- When a GW passes by an experimental $h^{\mathrm{exp}}(t)$ is recorded as a time series:

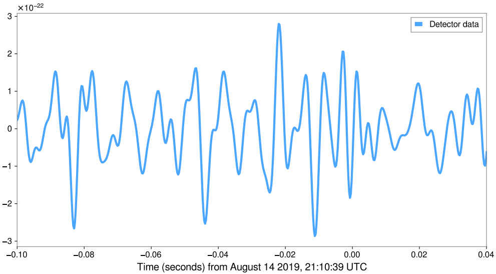

Figure: Filtered strain data of GW190814 from the LIGO-Livingston detector.

- Our theoretical prediction $h(t, \boldsymbol{\theta})$,

$$\boldsymbol{\theta} = (M_c,\ q,\ \chi_1,\ \chi_2,\ \theta_1,\ \theta_2, \phi_{12},\ \phi_{JL},\ \iota,\ \psi,\ \alpha,\ \delta,\ d_L), \qquad (2)$$

- Our theoretical prediction $h(t, \boldsymbol{\theta})$,

$$\boldsymbol{\theta} = (M_c,\ q,\ \chi_1,\ \chi_2,\ \theta_1,\ \theta_2, \phi_{12},\ \phi_{JL},\ \iota,\ \psi,\ \alpha,\ \delta,\ d_L), \qquad (2)$$

can then be used to fit $h^{\exp}(t)$:

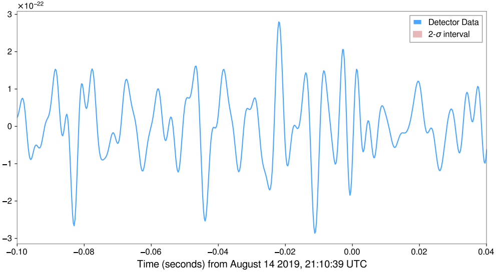

Figure: 2-σ confidence interval fit to GW190814.

- We can always consider a new theoretical strain $\bar{h}(t, \bar{\boldsymbol{\theta}})$

$$\bar{\boldsymbol{\theta}} \equiv (M_c,\, q,\, \chi_1,\, \chi_2,\, ,\, \ldots, \delta p), \tag{3}$$

which recovers GR at $\delta p = 0$ (null tests):

$$\bar{h}(t, \bar{\boldsymbol{\theta}})\Big|_{\delta p = 0} = h(t, \boldsymbol{\theta}). \tag{4}$$

- We can always consider a new theoretical strain $\bar{h}(t, \bar{\boldsymbol{\theta}})$

$$\bar{\boldsymbol{\theta}} \equiv (M_c,\, q,\, \chi_1,\, \chi_2,\, ,\, \ldots, \delta p), \tag{3}$$

which recovers GR at $\delta p = 0$ (null tests):

$$\bar{h}(t, \bar{\boldsymbol{\theta}})\Big|_{\delta p = 0} = h(t, \boldsymbol{\theta}). \tag{4}$$

- If GR is correct, one should find that $\delta p = 0$ is included in our error bars.

- We can always consider a new theoretical strain $\bar{h}(t, \bar{\boldsymbol{\theta}})$

$$\bar{\boldsymbol{\theta}} \equiv (M_c,\, q,\, \chi_1,\, \chi_2,, \ldots, \delta p), \tag{3}$$

which recovers GR at $\delta p = 0$ (null tests):

$$\bar{h}(t, \bar{\boldsymbol{\theta}})\Big|_{\delta p = 0} = h(t, \boldsymbol{\theta}). \tag{4}$$

- If GR is correct, one should find that $\delta p = 0$ is included in our error bars.
- Concretely, given the inspiral phase

$$\Psi(f) = 2\pi f\, t_c - \varphi_c - \pi/4 + \frac{3}{128\eta} \sum_{n=0}^{7} \left[\varphi_n + \varphi_n^{(l)} \ln(\pi M f)^{1/3}\right] (\pi M f)^{\frac{n-5}{3}},$$

- the modification is $\varphi_i \to (1+\delta p_i)\,\varphi_i$ for one φ_i at a time and the fit of $\bar{h}(t,\bar{\theta})$ to $h^{\exp}(t)$.

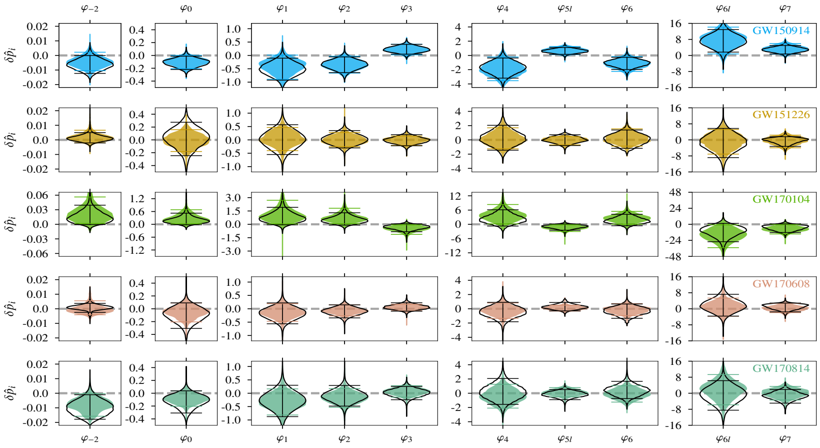

Figure: Posteriors for the individual binary black-hole events of GWTC-1 arXiv:1903.04467v3

- One may naturally be interested on the improvement of third generation detectors

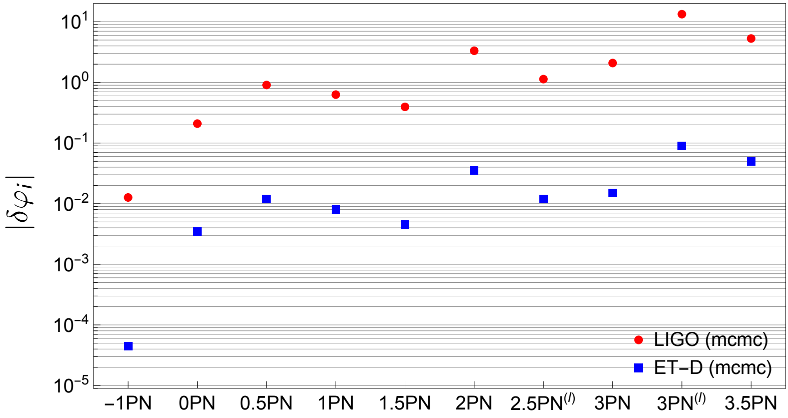

Figure: Bluebook (2503.12263) comparison of constraints on PPN parameters from LIGO (red) and ET (blue) for GW150914.

- Since we want to forecast, it is interesting to compare to the Fisher matrix

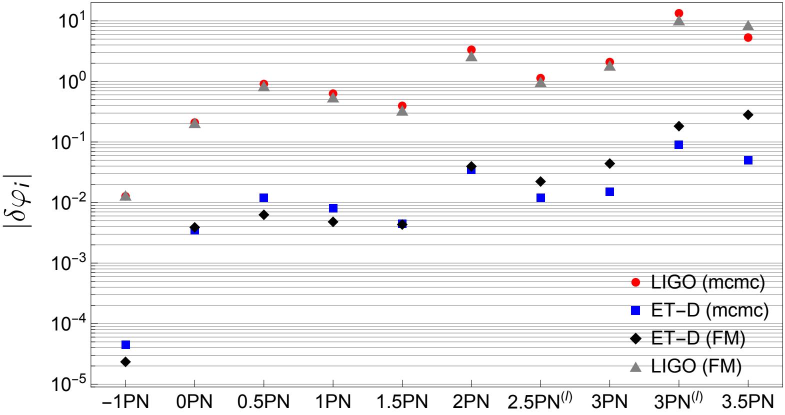

Figure: Comparison of constraints on PPN parameters from LIGO and ET including their Fisher matrix estimate.

- It is also interesting to check the impact of different ET designs

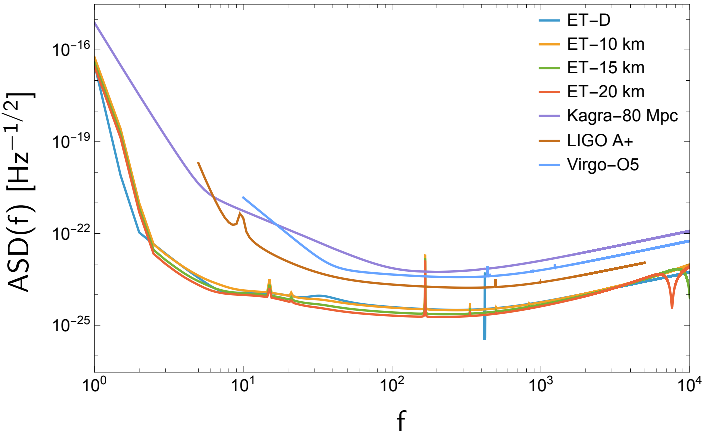

Figure: Amplitude spectral density from ET designs and LIGO, Virgo, Kagra expectations for O5.

- Considering a BBH population in agreement with GWTC-3, already at the SNR level one can see a considerable improvement:

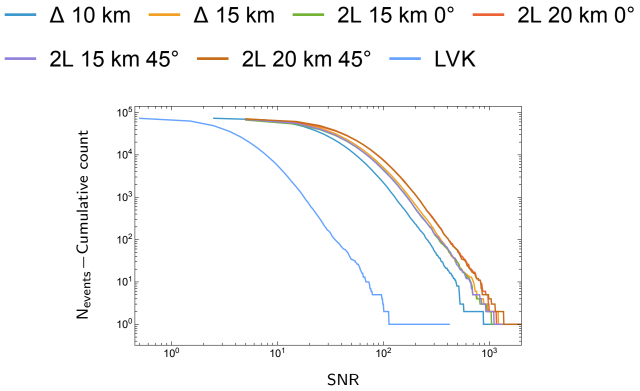

- Considering a BBH population in agreement with GWTC-3, already at the SNR level one can see a considerable improvement:

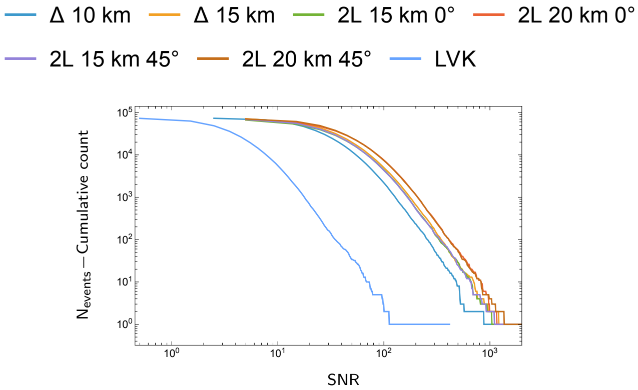

- In fact, with a detection threshold of 8, duty cycle of 0.85 and 74480 events (1 year of observations)

$$\text{LVK-O5: } 10788 \ (\approx 14.5\%) \tag{5}$$

$$\text{ET: } 68619 \text{ - } 72633 \ (\approx 92.1\% - 97.5\%) \tag{6}$$

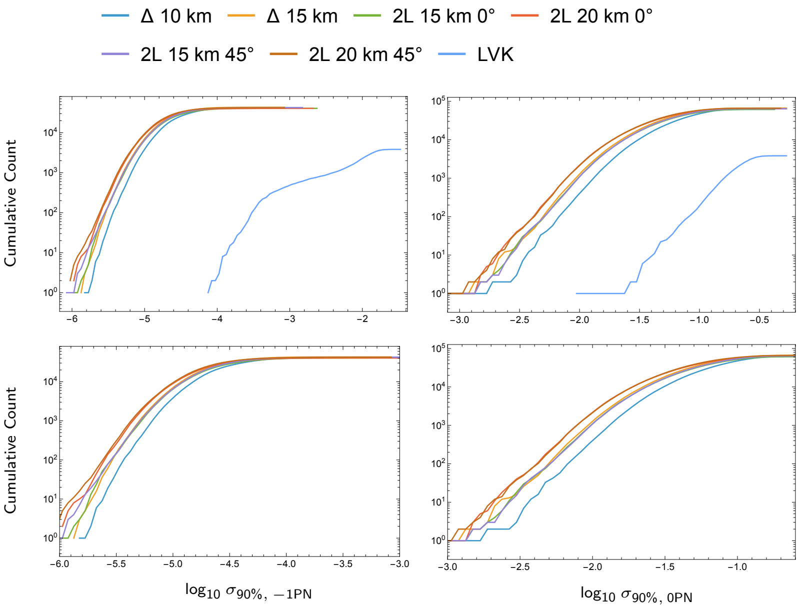

Δ 10 km
Δ 15 km
2L 15 km 0°
2L 20 km 0°
2L 15 km 45°
2L 20 km 45°
LVK
Cumulative Count
Cumulative Count
$\log_{10} \sigma_{90\%}$, −1PN
$\log_{10} \sigma_{90\%}$, 0PN

- We summarize the improvements by looking at the increase in the number of events with error bars smaller or equal to the mean of the T-10 km configuration:

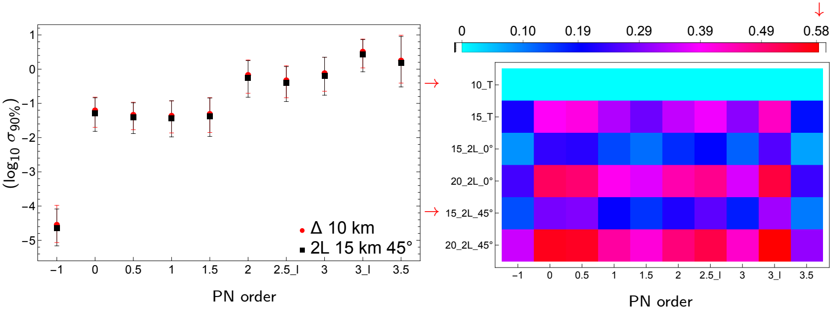

Figure: `Left` distribution of 90% confidence levels for different events in the population. `Right` improvement on the number of events detected with 90% confidence levels smaller or equal to the ones of the 10 km triangle

- And the improvements over the baseline get better if we consider only the 2351 golden events (SNR≥100) of the T-10 km:

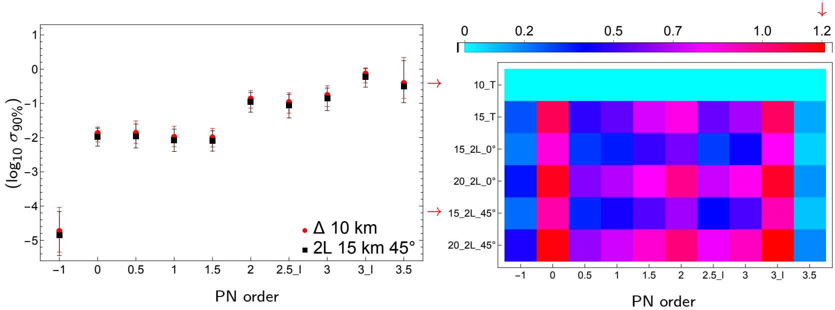

Figure: `Left` distribution of 90% confidence levels for different events in the population. `Right` improvement on the number of events detected with 90% confidence levels smaller or equal to the ones of the 10 km triangle

- ET performs considerably better than LVK;

- ET performs considerably better than LVK;
- however, there still considerable difference between networks;

- ET performs considerably better than LVK;
- however, there still considerable difference between networks;
- Our next step is to check the accuracy of this results against DALI, the higher order formalism of Fisher matrices

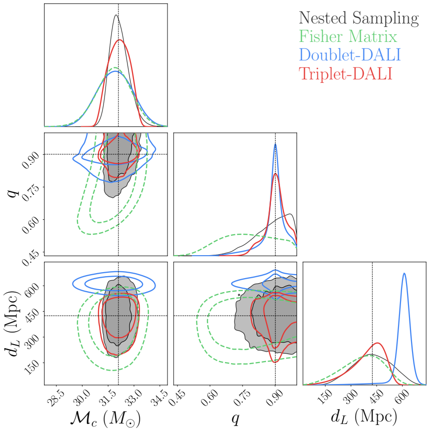

Figure: GW150914 (2203.02670)

Acknowledgements

- FAPES - Scholarship
- CPT-Aix-Marseille University Visiting Phd student.